Beyond Release: Development and Mechanistic Analysis Of A Performance Predictive Assay for Liposomal Prednisolone Phosphate

Shakti Nagpal[1], Jordan Png[1], Lyes Kahouadji[2], Matthias G Wacker[1,]*

[1] *National University of Singapore, Faculty of Science, Department of Pharmacy and Pharmaceutical Sciences, Singapore*

[2] *Department of Chemical Engineering, Imperial College London, South Kensington Campus, SW7 2AZ, London, United Kingdom.*

*Corresponding author:

Associate Professor Matthias G. Wacker
Department of Pharmacy and Pharmaceutical Sciences │ Faculty of Science
National University of Singapore
4 Science Drive 2
Singapore 117544
matthias.g.wacker@nus.edu.sg
Phone +65 6516 1133
Fax +65 6779 1554
www.thewackerlab.com

1. Abstract

Predictive performance assays are crucial for the swift development and approval of nanomedicines and their bioequivalent successors. At present, there are no established compendial methods that provide a reliable standard for comparing and selecting these formulation prototypes, and a comprehensive understanding of the relevant *in vivo* release conditions is still incomplete. Consequently, extensive animal studies, with enhanced analytical resolution for both, released and encapsulated drug, are necessary to assess bioequivalence. This significantly raises the cost and duration of nanomedicine development. The present work describes the development of a discriminatory and biopredictive release test method for liposomal prednisolone phosphate. A model-informed selection of target criteria for medium and test conditions was used. The experimental design involved a discreate L-optimal configuration to refine the analytical method. A three-point specification covered the most important phases of the *in vivo* release. The early (T-5%), intermediate (T-20%), and late release behavior (T-40%) were evaluated against the *in vivo* release profile of the reference product NanoCort®. Various levels of shear responses and the influence of clinically relevant release media compositions were tested. This enabled an assessment of the shear shielding effect of proteins on the release, an essential aspect of their *in vivo* deformation and release behavior. Fetal bovine serum had the strongest impact on the discriminatory performance at intermediate shear conditions. The method provided deep insights into the release response of liposomes and offers an interesting workflow for *in vitro* bioequivalence evaluation.

2. Keywords

Nanoparticles, Dissolution, Biopredictive, Biorelevant, Quality by design

3. Graphical Abstract

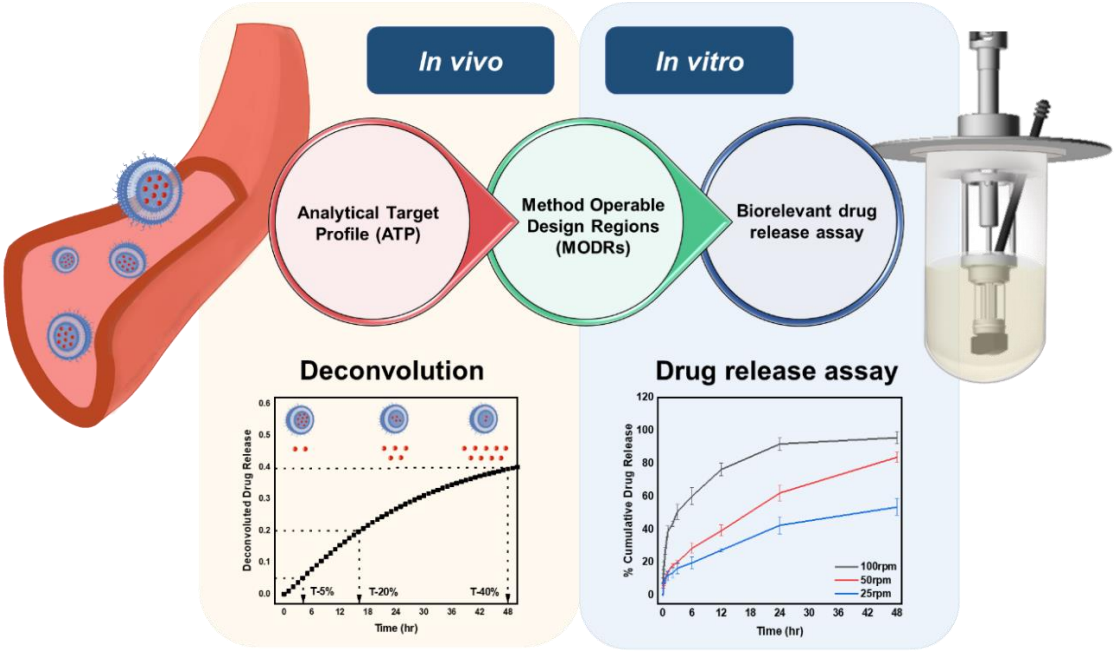

4. Introduction

Liposomes are lipid vesicles that encapsulate at least one aqueous compartment within one or more lipid bilayers [1,2]. In addition to phospholipids, additives such as cholesterol or surfactants can be added to alter the membrane structure and release behavior [3]. Variations in pharmaceutical quality including size, size distribution, surface charge, composition, and membrane fluidity, have been recognized to affect the pharmacokinetics (PK) of liposomes [4,5]. Therefore, comprehensive characterization of these attributes, along with the development of assays predictive of the *in vivo* performance, is crucial for creating safe and effective delivery systems [6–8].

Phase I clinical trials provide highly detailed information regarding dosage form performances. Plasma concentrations in a small patient population over time are more sensitive to changes in the physicochemical characteristics of the drug product than pharmacodynamic outcomes in Phase II-IV trials. Therefore, release test methods that mimic plasma release performance are most suitable for establishing clinically relevant conditions. To achieve this aim, a mechanistic understanding of the impact of *in vitro* parameters on the predictive capabilities of the assay is required [10,11]. Furthermore, release test methods with a high resolution for dosage form performances in physiological media are required.

Currently, there is no standard method for assessing the release kinetics of complex injectable formulations. Traditional dissolution technologies often fail to adequately correlate with *in vivo* release performances of liposomes [6,9,10]. Adjustments to these test conditions, such as hydrodynamics and media composition, can be made to enhance predictive accuracy. As per ICH Q14 guidelines, the development of a robust analytical methodology involves a systematic workflow. Firstly, the quality attributes of the delivery system must be identified, followed by the selection of appropriate technologies and their determination within the method-operable design regions (MODRs). The guideline recommends the implementation of multivariate experiments using Design of Experiments (DoE) to assess parameter ranges and potential interactions.

At present, a range of methods, including sample-and-separate, dialysis, and others, are utilized, tailored to the specific traits of the nanocarrier [9,11]. The analytical

method may systematically underestimate the release due to insufficient selectivity for the liposomes. A recent assay developed by the Nanoparticle Characterization Lab under the United States National Institute of Health introduced a separation method for liposomal doxorubicin that likely translates to other drug substances as well. It uses deuterated doxorubicin to distinguish between the encapsulated and non-encapsulated fractions. Still, for many approaches, issues arises particularly from the formation of larger protein complexes of the drug and analytical errors related to separation time [12]. Moreover, the adsorption of the analyte or analyte-protein complexes to membrane or column materials represents a common error source. These analytical inaccuracies undermine the predictive capability of the assay system and pose a significant threat to the quality of decision-making. Ultimately, such shortcomings may elevate the potential for safety risks. To enhance the accuracy and reliability of release estimations, it is imperative to address these challenges by refining the analytical methods to improve selectivity and mitigate kinetic errors, ensuring that the physiological triggers of release are accurately integrated without compromising the reproducibility and robustness of the *in vitro* release test method. These triggers can include, for instance, the diffusion of the drug through the bilayer membrane, disruption of the membrane due to ongoing degradation or exchange of phospholipids, as well as the effects of a high-shear environment and collisions of liposomes with other entities present in the bloodstream.

Dialysis-based methods are preferred for testing liposome release due to their efficacy in developing *in vitro-in vivo* relationships (IVIVRs) [7,8,13–17]. Several estimations integrate physiologically-based biopharmaceutics (PBB) models [8,18,19] to predict the PK of injectable drugs more accurately [20]. Regulatory authorities, including the US Food and Drug Administration (FDA) and the European Medicines Agency (EMA), generally support the computational analysis and development of *in vitro-in vivo* correlations (IVIVCs) [21] and, in particular, for the evolving field of complex injectables to enhance dossier submissions. Additionally, these agencies are advocating for the development of *in vitro-in vivo* correlations (IVIVCs) for complex injectable drugs to aid in dossier submissions [19,22].

Traditional deconvolution methods often inadequately estimate absorption kinetics from liposomal systems [8,23]. Our predictive Design Coversed Optimization and Deconvolution (DeCODe) model [13,17,20] addresses this gap by extending to

prednisolone phosphate liposomes and establishing *in vitro* release specifications across the drug delivery lifecycle. This current work compares the *in vitro* and *in vivo* release kinetics, systematically altering the *in vitro* test conditions. This enables a better understanding of the mechanistic relationships underlying *in vitro* release and the biopredictive capabilities of the assay. Release specifications are based on the early, intermediate, and late phases of the drug delivery lifecycle which are essential for successful delivery.

5. Materials and methods

5.1 Materials

Disodium prednisolone phosphate was purchased from Cayman Chemical (Michigan, USA). Prednisolone (P) and Cholesterol were purchased from Sigma-Aldrich (Singapore). For liposome preparation, the lipids DPPC and DSPE-PEG-2000 were purchased from Lipoid GmbH (Ludwigshafen, Germany). Spectra/Por® Biotech cellulose ester (CE) dialysis tubing with molecular weight cut-offs (MWCO) of 50 kDa and 300 kDa and with a flat width of 31 mm were purchased from Spectrum Labs (Rancho Dominguez, USA). Bovine serum albumin (BSA), fetal bovine serum (FBS), and Penicillin streptomycin (Penstrep®) solution were purchased from Biowest (Missouri, USA). The Pharma Test Dispersion Releaser (PT-DR) devices were kindly provided by Pharma Test (Hainburg, Germany). All other reagents were of analytical or high-performance liquid chromatography (HPLC) grade.

5.2 Preparation and characterization of liposomes

The batches of Prednisolone Phosphate-loaded liposomes were manufactured using film hydration followed by extrusion as described by Metselaar et al [24]. In summary, an ethanolic solution of the lipids (DPPC, DPSE-PEG2000, and cholesterol at a 1.85 : 0.15 : 1.0 molar ratio), was dried using a rotary evaporator to form a thin film. After the hydration of the film with an aqueous prednisolone phosphate solution (100 mg/mL), lipid self-assembly, and co-encapsulation of the drug, repeated extrusion steps were performed using polycarbonate membranes. The free drug was removed at 4°C by dialysis against PBS (10mM, pH 7.4). The resulting liposomes were diluted 5000-fold and characterized for their size by dynamic light scattering (DLS) using a Litesizer™ 500 (Anton Paar GmbH, Graz, Austria) at 25°C and a detection angle of 173° in plastic disposable cuvettes. The zeta potential was also measured using the same system in Omega cuvettes. Additionally, the particle size distribution in PBS and varying concentrations of FBS was determined by nanoparticle tracking analysis (NTA) at 25°C using a Nanosight NS 300 (Malvern Instruments, Malvern, UK). The encapsulation and loading were determined by high performance liquid chromatography (HPLC).

5.3 Analytical methodology

The HPLC system (Chromaster, VWR Hitachi, Tokyo, Japan) included a DAD detector (5430), a pump (5160), an autosampler (5260), and a column oven (5310). A reverse phase C18 column (Gemini® NX C-18, Phenomenex Ltd., Aschaffenburg, Germany) with specifications of 150 x 4.6 mm, pore size 110 Å, particle size 5 µm and mounted with a pre-column of the same material were used as stationary phase. A constant column temperature of 35°C, was maintained throughout the analysis. The mobile phase consisted of acetonitrile, water, and trifluoroacetic acid (TFA) at a volume ratio of 25:75:0.1 and the flow rate was set to 1 mL/min. Prednisolone phosphate was extracted from the biological matrix (FBS and BSA solutions) through protein precipitation followed by evaporation using a TurboVap® (Caliper Life Sciences, Hopkinton, USA) under a continuous 10 psig stream of nitrogen and at a bath temperature at 40°C. The dried samples were reconstituted with mobile phase followed by analysis. All measurements were conducted in triplicates.

5.4 Release conditions

Before the release study, the *in vitro* parameters were carefully selected. To mimic the physiological conditions, PBS, (10mM, pH 7.4) alone or supplemented with FBS in varying concentrations (10%, 50%, and 90% v/v) were used. To assess the influence of albumin specifically, PBS, (10mM, pH 7.4) was supplemented with BSA in concentrations, of 4 g/L, 20 g/L, and 35 g/L. The influence of hydrodynamics was systematically tested varying the shear stress using 25rpm, 50rpm, and 100rpm. These parameters were set as independent variables using a custom L-optimal design in Design Expert v13.0 (Stat-Ease, Inc., Minnesota, USA).

To assess the influence of the buffer on the release, a 10mM 4-(2-hydroxyethyl)-1-piperazineethanesulfonic acid (HEPES) buffer supplemented with 143 mM sodium chloride was adjusted to a final osmolarity of 295 mOsmol/kg and pH 7.4.

5.5 Performance testing

5.5.1 Chemical stability of drug

The drug conversion of prednisolone phosphate to prednisolone was evaluated in the presence of different concentrations of FBS. The experiments were conducted at 37 ± 0.5°C using a USP dissolution apparatus II (Pharmatest Apparatebau AG, Hainburg, Germany) and a stainless steel PT-DR setup with mini-vessel configuration.

An adequate volume of prednisolone phosphate solution corresponding to an absolute dose of 365 µg was diluted with a relevant volume of test media and injected into the donor chamber. The acceptor chamber was filled with 114mL of dissolution medium. The donor chamber was sealed with a CE membrane (300kda) using O-rings, and punctured with a surgical blade. A total volume of 3 mL was added into the donor chamber using a 70 mm needle (B Braun, Melsungen, Germany). Samples (0.3 mL) were collected at 0.08, 0.16, 0.25, 0.5, 1, 2, 3, 6, 12, 24, and 48 hr, with similar volumes being replenished using fresh media. The collected samples were immediately diluted with the 3-fold volume of acetonitrile and vortexed, centrifuged at 4°C, at 12,000 × g for 10 min. Carefully collected supernatant was evaporated in a continuous stream of nitrogen (flow gradually adjusted to 10 psig) at 50°C water bath temperature. The tubes were resuspended with 150µL of mobile phase, vortexed, and centrifuged in the same way described above. The supernatant (125µL) was added to HPLC inserts and injected into the system.

5.5.2 Stability of Liposomes in release media

A dose of liposome corresponding to 365.41 µg of prednisolone phosphate , diluted to 3mL with release media, was added to the donor compartment of the PT-DR setup using a 5 mL syringe (Terumo Corporation, Tokyo, Japan) equipped with a 70mm needle (B Braun, Melsungen, Germany). The acceptor chambers consisted of mini vessels filled with 114 mL of test media. The entire setup was placed in a USP dissolution tester (Pharma Test, Apparatebau AG, Hainburg, Germany) and maintained at 37°C throughout the experiment. At 24hr intervals, a 20µL sample was drawn from the donor chamber using an 80mm needle (B Braun, Melsungen, Germany) attached to a 1mL syringe (Terumo Corporation, Tokyo Japan). The size of these 1000x diluted samples was then characterized by the Nanosight NTA300 (Malvern Panalytical Ltd, Malvern, UK), normalized against a background of agglomerates from the media.

5.5.3 Membrane permeation testing

Membrane permeation studies for prednisolone phosphate were carried out in various media compositions. The PT-DR setup mounted on a USP-II dissolution tester, (Pharma Test, Apparatebau AG, Hainburg, Germany), equipped with an intact CE membrane (50kDa and 300Kda), was arranged as previously mentioned. A dose

equivalent to 365µg of prednisolone phosphate solution was diluted with release media to a total volume of 3mL and injected into the donor compartment. Regular sampling (0.3mL) was performed at time points of 0.08, 0.16, 0.25, 0.5, 1, 2, 3, 6, 12, 24, and 48hr.The samples were processed immediately, following the earlier described procedure.

5.5.4 Drug release testing

The drug release study was conducted in a stainless-steel PT-DR setup set as described above. A Liposome dose corresponding to 365.41µg prednisolone phosphate and diluted to 3mL with relevant release media, was added to the donor compartment using a 5mL syringe (Terumo Corporation, Tokyo, Japan) mounted with a 70mm needle (B Braun, Germany). The acceptor chamber was filled with 114mL relevant media and the whole setup was mounted on a USP dissolution tester (Pharma Test, Apparatebau AG, Hainburg, Germany), maintained at 37°C for the whole duration of the experiment. The shear was varied according to the discrete combination of design varying shear stress from 25- 100rpm. At regular intervals of 0.08, 0.16, 0.25, 0.5, 1, 2, 3, 6, 12, 24, and 48 hours, with equal volume replacement using fresh media. The samples were processed immediately, as described above before injecting to HPLC for quantification.

5.5.5 Estimation of the wall shear

The PTDR uses a rotating paddle stirrer to accelerate the membrane transport of drugs and reduce the interaction with medium components during the release test In the current investigation, quantifying the shear rate exerted on the dosage form was necessary. For this purpose, we assume a pure shear flow without vortical structures during the stirring process. Therefore, both radial and axial velocity components can be neglected compared to its azimuthal component which is used here to quantify the wall shear. Assuming a non-slip condition for the fluid at both the rotating paddle and the motionless inner wall of the donor chamber, the azimuthal velocity profile decreases linearly from its maximum value at the tip of the paddle toward zero at the inner wall , where the maximum value of the wall shear is expected and is estimated using the following equation 1:

$$\tau_w = \mu * \frac{2\pi R f}{\Delta r} \qquad 1$$

Here, the wall shear (τ_w) is defined using the azimuthal velocity of the rotating paddle blade ($v_\theta = 2\ \pi\ R f$), with (R) the radius, (f) the frequency, and divided by the gap size (Δr) between the paddle blade and the inner donor chamber wall. Finally, (μ) refers to the dynamic viscosity which is assumed to be constant for each release medium.

5.6 Modeling pharmacokinetics of Liposomal Prednisolone Phosphate

5.6.1 Data extraction, software and statistics

Literature data for rat PK profile following a single 5mg/kg intravenous dose of prednisolone phosphate in liposomal and drug solution was and digitized using Graph Grabber (v2.0.2, Quintessa, © 2017, Henley-on-Thames, UK). The respective compartmental model was developed and analyzed for sensitivity and statistics using Stella® Architect (v3.3, isee systems, Lebanon, USA) and MonolixSuite 2019R2 (Lixoft, Antony, France). The graphs were plotted with OriginPro 2019 (OriginLab Corporation, Northampton, USA).

5.6.2 Modeling pharmacokinetics of liposome-associated and free drug fractions

The multi-compartment model was based on Nagpal et al. 2023 [8] and designed using Stella Architect (v3.0.1, isee systems, Lebanon, USA). To estimate plasma release and carrier elimination rate, the extracted data from Metselaar et al [24] was analyzed using the PBNB model coded in Mlxtran (MonolixSuite 2019R2, Lixoft, Antony, France). The multi-compartment model comprises a carrier compartment with the volume of distribution V_{DC}. V_{DC} is assumed to be the physiological plasma volume of the respective species. The carrier circulation half-life (HL) was calculated as per equation 2.

$$\boldsymbol{K_{CA} = 2.303 \times \left(\frac{Log(2)}{HL}\right)} \qquad 2$$

The fraction of the drug released over time, denoted as F, is estimated using the 3RPT model, as shown in equation 3.

$$\boldsymbol{F = \left(\frac{t^b}{t^b + m}\right) \times c} \qquad 3$$

The drug release rate, K_{rel}, is derived from the first derivative of the 3RPT model, as indicated in equation 4.

$$K_{rel} = \frac{dF}{dt} = m \times b \times c \times \left(\frac{t^{b-1}}{(t^b+m)^2}\right) \quad (4)$$

Following its release, prednisolone phosphate is rapidly dephosphorylated. This process is modeled using a first-order conversion process. The parameter ranges obtained during the model analysis have been summarized in **Table 1**.

Table 1 Parameters and corresponding ranges utilized in the *in silico* modeling.

Formulation and study design	Parameter	Initial value	Range	Reference
Prednisolone phosphate incubated with murine phosphatase	k (h^{-1})	8.22	7-10	[25]
Prednisolone (Prednisolone phosphate solution (5 mg/kg) in male Lewis Rats)	V_{DF} (mL)	1295.64	841.38-1869.9	[24]
	K_{12} (h^{-1})	0.677	0.547-0.766	
	K_{21} (h^{-1})	0.732	0.592-0.865	
	k_{FE} (h^{-1})	1.06	0.7-1.39	
	F_{liver} (%)	2.551	2.377-2.725	[26]
Physiological parameters for PBPK modelling	F_{RBV} (liver)	0.21	0.12-0.27	[27]

Furthermore, physiologically based parameters were integrated to simulate the liver disposition. The previously published PBNB model [20] was extended with multiple compartments. Since the organ levels of prednisolone after injection of the liposomes were unavailable, liver distribution parameters of the liposomes were adopted from liposomal doxorubicin. The liposomal formulations are identical in composition and vary in their payload only. The influx and outflux from and into the liver (KL_{in}, KL_{out}) were calculated using the literature data summarized in

296 Table 2.

297

Table 2: Parameters used in computing hepatic distribution of free prednisolone

Parameter	Initial value	Range	Reference
Relative Q_H (%)	17.4	13.1-22.4	[27]
Cardiac output (ml/hr)	6624	5040-8040	
Liver tissue density (g/ml)	1	-	
R_b	0.703	0.693-0.713	[28]
K_d (µg/ml)	0.00301	0.00229-0.00373	
B_{max} (µg/ml)	0.1885	0.1666-0.2104	
f_u	0.6	-	

KL$_{in}$ was calculated by the following series of equations, which considers liver perfusion (Q_H), fraction unbound of prednisolone (f_u), and blood-to-plasma concentration ratio of prednisolone (R_b). To find the hepatic perfusion rate, it was calculated as a function of cardiac output in equation 5:

$$\boldsymbol{Q_H}(\boldsymbol{ml.hr^{-1}}) = \boldsymbol{Relative\ Q_H}\ (\%) \times \boldsymbol{Cardiac\ output}\ (\boldsymbol{ml.hr^{-1}}) \quad 5$$

As per the free hormone hypothesis, the free hormone is the entity participating in interactions with biological membranes in drug distribution, therefore in unbound concentration of prednisolone in blood ($C_{u,b}$) has to be considered. Since f_u and R_b of prednisolone are known [29], the fraction unbound of prednisolone in blood can be calculated by equation 6, as measured unbound concentration in whole blood and plasma is equivalent.

$$\boldsymbol{f_{u,b}} = \left(\frac{\mathbf{1}}{\boldsymbol{R_b}}\right) \times \boldsymbol{f_u} \quad 6$$

The concentration of prednisolone in blood, (C_b) is calculated by the product of R_b and plasma concentration of prednisolone (C).

$$\boldsymbol{C_b} = \boldsymbol{R_b} \times \boldsymbol{C} \quad 7$$

The unbound concentration of prednisolone in blood ($C_{u,b}$) is determined using equation 7:

$$\boldsymbol{C_{u,b}} = \boldsymbol{f_{u,b}} \times \boldsymbol{C_b} \quad 8$$

The rate of liver presentation, K_{Lin} is subsequently computed by the product of equations 5 and 8 as presented in equation 9.

$$K_{L_{in}} = Q_H \times C_{u,b} \quad (9)$$

In a recent study published by Li et al., ratio of total to unbound drug concentration in tissues ($K_{p,u}$), was determined using equation 10.

$$K_{p,u} = \frac{-(C_t - K_d - B_{max}) + \sqrt{(C_T - K_d - B_{max})^2 + 4K_d C_T}}{2K_d} \quad (10)$$

C_t is the total concentration of prednisolone in tissue, K_d is the prednisolone-tissue dissociation rate constant and B_{max} is the binding capacity of the tissue for prednisolone. Equation 11 that describes the non-linear tissue binding of prednisolone [29].

$$C_T = C_{uT} + \frac{B_{max} \times C_{uT}}{K_d + CuT} \quad (11)$$

The Unbound concentration of prednisolone in the tissue (C_{uT}) is obtained using equation 12 accordingly.

$$C_{uT} = \left(\frac{C_T}{K_{p,u}}\right) \quad (12)$$

The liver-specific values of K_d and B_{max} are summarized in

Table 2. $K_{L\text{-}out}$ calculated as follows:

$$K_{L_{out}} = Q_H \times C_{uT}(Liver) \quad (13)$$

According to the literature, the accumulation of nanoparticles mediated by macrophages leads to their disposition primarily in the organs of the RES, such as the liver and spleen. Therefore, the carrier accumulation, denoted as K_{CA}, is assumed to be a first-order rate of accumulation into the RES system. The fraction of nanoparticles disposed of by macrophages is modeled by assigning a Liver Fraction (LF). This fraction modulates both hepatic (K_{LA}) and extra-hepatic accumulations (K_{EHA}). The relationship between these factors and the overall accumulation and disposition process in the MPS system is described by equations 14 and 15 as below.

$$K_{LA} = LF \times K_{CA} \quad (14)$$

$$K_{EHA} = (1 - LF) \times K_{CA} \quad (15)$$

As outlined previously, K_{CA} was adopted form pegylated liposomal doxorubicin by Siegal et al. [30], assuming similar disposition performance of carrier by liver and to circumvent the lack of biodistribution data for liposomal prednisolone phosphate.

5.6.3 Influence of prednisolone dephosphorylation

Assuming rapid dephosphorylation of prednisolone phosphate, the released fraction of the drug can be estimated from the prednisolone concentrations found in the blood plasma. Hence, further investigations were conducted to accurately model the dephosphorylation rate and account for the error arising from a misprediction.

Previous works reported that liposomal encapsulation inhibits the dephosphorylation of prednisolone phosphate to prednisolone by the phosphatases present in the blood plasma [24,25,31]. Metselaar et al. [24], for instance, highlighted that no free prednisolone phosphate could be detected in plasma within one hour of administration. However, this rate of dephosphorylation in rats has yet to be adequately characterized in the literature [25,32]. Smits et al. [32] assumed the dephosphorylation rate to be instantaneous based on findings from an *in vitro* investigation on murine phosphatases. To ensure the robustness of the *in silico* model developed for prednisolone phosphate, an intermediate compartment representing released prednisolone phosphate, between encapsulated prednisolone phosphate and

dephosphorylated prednisolone in both plasma and liver, was factored in. In the absence of dephosphorylation data in rats, this was approximated in the model by taking the plasma half-life of prednisolone phosphate as reported by Metselaar et al. [24] and estimating rodent phosphatase activity from dephosphorylation rates of murine phosphatases as reported by Smits et al. [32,33]. To account for uncertainty, an optimization was performed within the concentration ranges found in the blood plasma. This optimization provides potential local or global optima defined by these plasma levels. Additionally, the dephosphorylation kinetics was included in the PPSA (refer to **Supplementary Materials, section S1**).

5.6.4 Statistical analysis of model fits

To compare the model predictions to the observations, the absolute average-fold error AAFE [34] was calculated using equation 16

$$\boldsymbol{AAFE} = \mathbf{10}^{\frac{\mathbf{1}}{\boldsymbol{n}}\times\boldsymbol{\Sigma}\left(\left|\boldsymbol{Log}\left(\frac{\boldsymbol{Pred,t}}{\boldsymbol{Obs,t}}\right)\right|\right)} \qquad 16$$

The absolute difference of predicted (Pred,t) and observed (Obs,t) plasma concentrations at time t are calculated. n represents the size of the dataset. An AAFE of ≤ 3 is has been often used as a threshold value to identify successful simulations [20,34–36].

5.6.5 Partial Parameter Sensitivity Analysis

Partial parameter sensitivity analysis (PPSA) using the sensitivity analysis mode of Stella® Architect was performed (discussed in the **Supplementary Materials, section S1**). With respect to the primary objective of this investigation, the PPSA was focused on liver-related drug distribution processes (i.e. the accumulation rate, carrier sequestration rate, and free drug hepatic influx and efflux rates). The drug release rate, in addition to the liver-related processes, was varied within a range of ±50% to assess the impact of uncertainty in model parameters on simulations executed using the model [37].

6. Results and discussion

Since the 1950s, pharmaceutical scientists have aimed to correlate *in vitro* dissolution data with *in vivo* performance, a challenge intensified by complex drug products [6]. Central to this effort are two pivotal strategies: the use of advanced deconvolution techniques for estimating *in vivo* release [8,13,17,38], and the design of *in vitro* models that accurately represent the release mechanism. This requires careful consideration of hydrodynamics, media composition, and physiological environment aspects, which are difficult to replicate *in vitro* [10,39]. Upon injection, nanocarriers encounter a dynamic environment characterized by varying mechanical shear and physiological conditions, essential to the lifecycle of liposomes. This environment significantly influences their *in vivo* characteristics, resulting in continuously evolving post-injection behavior. Although dialysis-based methods are favored, their sensitivity is often compromised by membrane permeation kinetics [6,11]. This study introduces the PT-DR technology combined with a validated PBB modeling framework tailored for liposomal drugs, enhancing the development of IVIVCs through a Quality-by-Design (QbD) approach.

6.1 Modelling disposition of liposomal prednisolone phosphate

The compartmental model used for PK deconvolution was adapted from a previously validated framework [8,20], with minor modifications for analyzing the investigational drug product NanoCort® (refer to **Figure 1a**) [24]. Several quality parameters indicated an optimal model fit including an AAFE<3 ($AAFE_{Carrier}$=1.23) [40], as well as the overlay of observed and predicted plasma profiles presented in **Figure 1b and c**. They highlight the plasma concentration-time profiles of prednisolone phosphate (**Figure 1b**) and prednisolone (**Figure 1c**), the main metabolite of the drug. Key assumptions of this prediction include a consistent biopharmaceutical behavior of liposomes regardless of their payload with the biodistribution pattern being primarily determined by the composition and structure of the lipid bilayer, rather than the drug molecule embedded into the aqueous core. Another crucial assumption is that the liposomal drug predominantly resides in the vascular system, from which prednisolone phosphate is distributed to various organs through extravasation and release. The distribution rates were verified using *in vivo* PK data obtained from the literature (refer to **Figure 1a and b**).

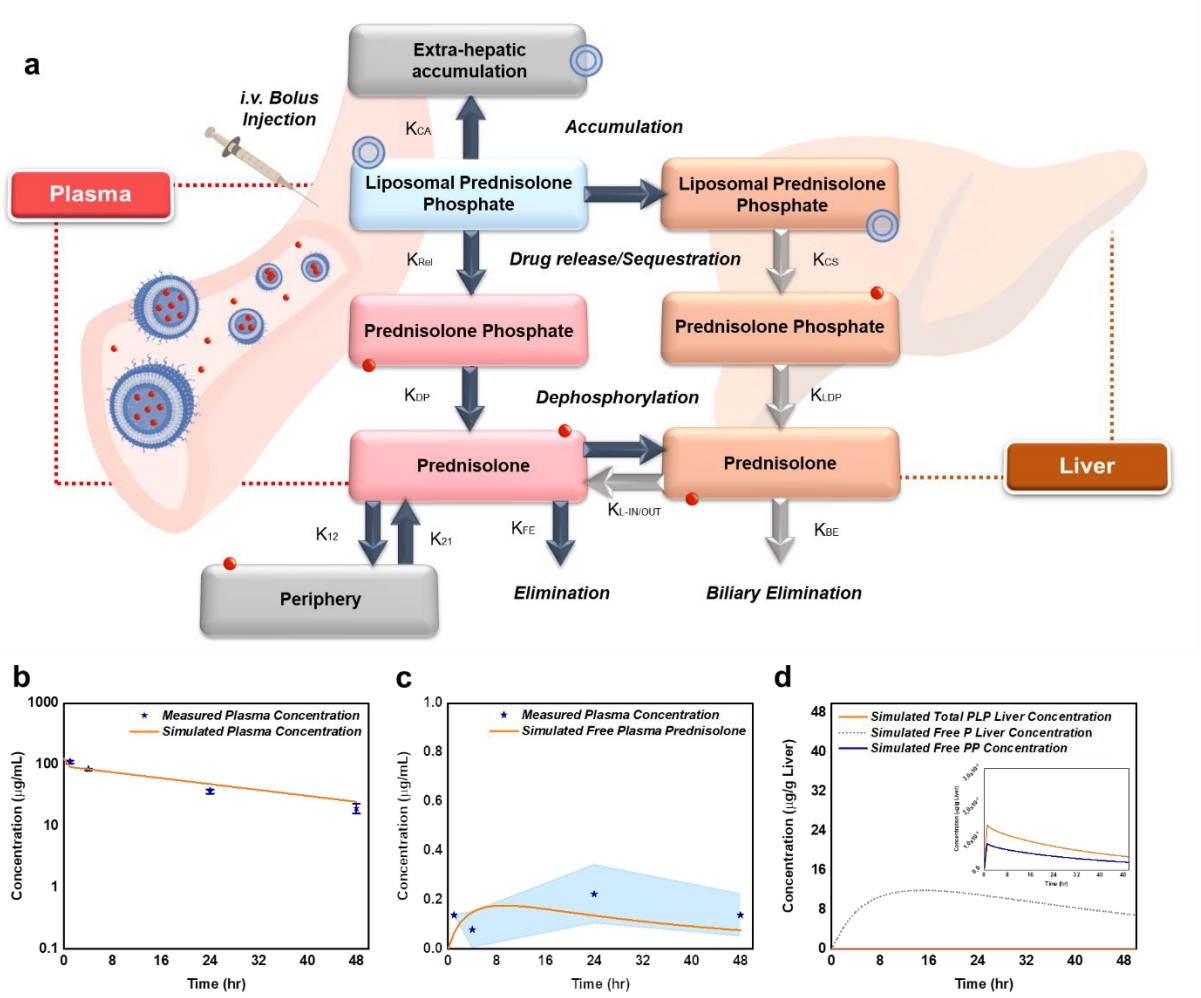

Figure 1. Graphical schematic of the *in silico* multi-compartmental model (A). The model consists compartments representing the carrier and the released fraction of the drug in the central and liver including the extra-hepatic accumulation of the carrier fraction and distribution of the free drug into the periphery compartment. Simulated (in orange) plasma concentration-time profiles of Liposome-bound prednisolone phosphate (B) and free Prednisolone (C) compared against measured (in blue stars) plasma concentration-time profiles respectively with mean and standard deviation represented by blue shaded area. Simulated liver concentration-time profiles of liposomal bound Prednisolone phosphate (D) and free Prednisolone (D).

In clinical settings, the release in the plasma commonly represents the only accessible *in vivo* data and is, therefore, better suited for establishing a relationship between *in vitro* and *in vivo* data. The dephosphorylation of prednisolone phosphate was simulated using accessible *in vivo* data reported by Smits et al. [32]. The phosphorylation rate must be considerably higher than the estimated release rate to avoid uncertainties in the release estimation.

This was confirmed by both literature data and our own ex vivo investigations in rat plasma (data not shown). Furthermore, we investigated the influence of dephosphorylation kinetics in the PPSA (refer to **Supplementary Materials, section S1**) and confirmed that even considerable misprediction (± 50%) does not undermine

the current simulation. In the following, the PK parameters derived from the DeCODe model were systematically used to compare *in vitro* profiles with *in vivo* estimations as described in more detail in section 6.2.

6.2 Model deconvolution

Originally developed to characterize the release from solid oral dispersions in quality control scenarios, the RPT equation effectively accommodates diverse release curves. In the current study, the 3RPT model, an adaptation that includes release rates under non-sink conditions, was utilized for the *in silico* simulation of drug release behavior from liposomal prednisolone phosphate. The parameters 'm' and 'b' define the shape of the release profile, while a third parameter, 'c', accommodates simulations of dissolution processes under non-sink conditions. All three parameters are reported in **Table 3**.

Table 3 PK parameters are estimated by the DeCODe model using differential evolution. AAFE and individual predictions confirmed the reliability of these estimations.

Referenced study	Formulation	Parameter	Value
Metselaar et al	Prednisolone in plasma (Dephosphorylated Prednisolone Phosphate (5mg/kg) in solution)	k_{12} (h^{-1})	0.569
		k_{21} (h^{-1})	0.852
		V_{DF} (mL)	842
		k_{FE} (h^{-1})	0.712
		$T_{1/2}$ (Free prednisolone phosphate) (h)	0.004
	Liposomal Prednisolone Phosphate (5mg/kg) in solution	$T_{1/2}$ (Liposomal prednisolone phosphate) (h)	24.6
		V_{DC} (mL)	8.95
		Liver Fraction	0.198
		k_{LA} (h^{-1})	0.00563
		k_{CS} (h^{-1})	0.81
		k_{LDP} (h^{-1})	9.76
		m	903
		b	0.0222
		c	0.443
		AAFE(Carrier)	1.23
		AAFE(Free)	1.12

The predicted *in vivo* drug release profile (refer to **Figure 2**) was coherent with the release behavior expected of stealth liposomes [3,24].

Still, the released fraction was higher than observed for similar formulations, such as Doxil®. At first glance, and based on the preclinical and clinical data, the release of prednisolone phosphate from the liposomes might appear insignificant due to the

absence of high concentrations of prednisolone phosphate or prednisolone in the blood plasma. However, this is explained by the rapid dephosphorylation of prednisolone phosphate and the 100-fold higher volume of distribution of prednisolone. Nonetheless, the formulation exhibits prolonged circulation and controlled release behavior [3,20]. This was further corroborated by the carrier half-life of 24.6 hrs as originally published by Metselaar et al [24].

After accounting for the effects of dephosphorylation and distribution, the deconvoluted release profile acts as a preclinically justified target for dissolution specifications, enabling a systematic comparison between *in vitro* release profiles and realistic estimations of *in vivo* release. However, the chosen methodology should not only reflect the rate and extent of release but also replicate similar release mechanisms. To highlight the sensitivity of the model to the individual model parameters, a PPSA was conducted and added to the ***Supplementary Materials, Section S2***.

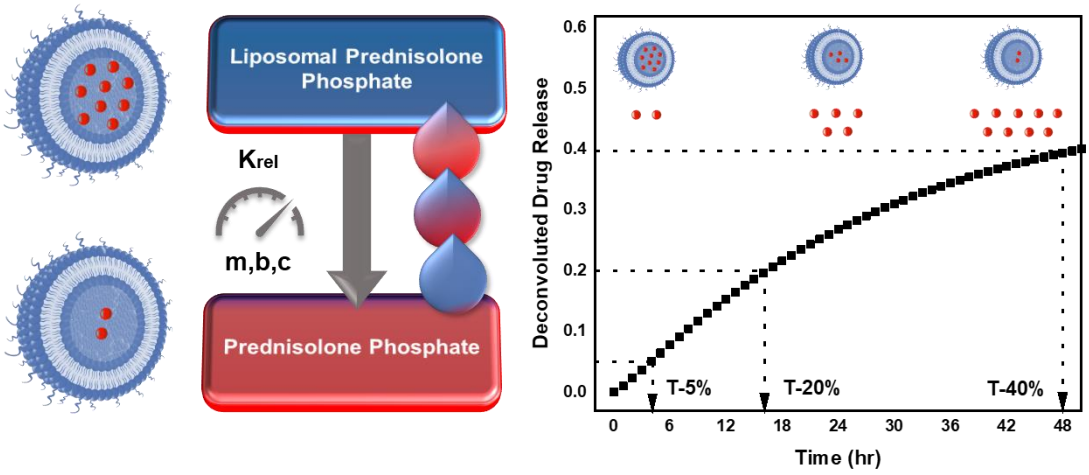

Figure 2 Deconvoluted drug release profile representing T-5%, T-20% and T-40%.

The release mechanism of prednisolone phosphate from NanoCort® is likely influenced by the concentration gradient between the aqueous core and the bloodstream, particularly during the initial minutes post-injection. It reaches a total release of more than 40% within 48 hrs. Model analysis confirms that more than 5% of prednisolone phosphate is released within the first 6 hours post-injection. The rate-limiting step and primary mechanism of release, however, is the permeation of the drug through the bilayer membrane. Therefore, membrane integrity plays a crucial

role. This integrity depends on the presence of serum lipases and acceptor molecules like albumin, which solubilize phospholipid components of the membrane [41], as well as the shear stress the liposomes are exposed to during circulation. Accordingly, the complex interplay between the protein type, concentration, and shear stress was a key aspect of this investigation.

Given the prolonged circulation time and the impact of gradual disintegration processes on layer permeability, the study systematically examined the correlation between release performance at early (T-5%), intermediate (T-20%), and late (T-40%) stages of release and the *in vivo* release profile.

6.3 Stability features of NanoCort®

To complement the *in vitro* release measurements, we evaluated the chemical stability of prednisolone phosphate across various release media and analyzed the plasma protein binding kinetics of prednisolone, the primary metabolite of the drug. This analysis aimed to estimate the impact of serum on drug degradation, solubilization, and distribution kinetics. Additionally, the physical stability of the liposomes was assessed under conditions of low shear.

6.3.1 Chemical Stability of Prednisolone Phosphate

The PT-DR is a dialysis-based setup that enables the testing of dispersed dosage forms, providing an accurate separation of the nanoparticle fraction from the dissolution media. It consists of a cylindrical donor compartment containing the substance to be tested, while the dissolution vessel forms the acceptor compartment. A dialysis membrane acts as a barrier between the donor and acceptor compartments. A small paddle stirrer in the donor compartment allows for precise control of shear forces within the donor compartment. A schematic of the PTDR has been included in the **Supplementary Materials, Section S2**.

A solution of prednisolone phosphate was exposed to FBS-supplemented media in a PTDR release assay to evaluate the degradation of prednisolone phosphate into prednisolone. Under high shear conditions, proteins and enzymes are more likely to reflect the expected real-time metabolism. As anticipated, the rate of prednisolone formation was highest in release media supplemented with 90% (v/v) FBS, followed by 50% (v/v) FBS, and then 10% (v/v) FBS, as shown in **Supplementary Materials,**

Figure S3. The chemical stability data contribute an additional dimension to the analysis of release performances, enabling a sensitive distinction between the release and conversion processes of prednisolone phosphate. The observed conversion of the drug, especially at high FBS concentration, suggests further metabolic breakdown of prednisolone into its metabolites. This underscores the analytical challenges associated with accurately quantifying the released drug *in vitro* and *in vivo*. This challenge was addressed using an integration of the *in vivo* conversion rates into the DeCODe model.

6.3.1 Membrane Permeation and Plasma Protein Binding Kinetics

Like most dialysis setups, the membrane permeation kinetics of drugs in the PT-DR depends on the material attributes as well as the MWCO of the membrane. Furthermore, interactions between the medium and the membrane may occur. The elevated shear rate in the donor compartment of the PT-DR reduces membrane adsorption and, consequently, the analytical error arising from a prolonged separation of the free drug from the dosage form. However, a certain delay due to membrane permeation is to be expected. To account for issues, drug permeation was measured under various conditions, determining the permeation in the absence and presence of various protein concentrations (refer to Table 4). This lays the groundwork for understanding the role of proteins in the drug release behavior of liposomal prednisolone phosphate.

The formation of a protein corona plays a key role in the disposition kinetics of nanomedicines. The effect of proteins, however, extends beyond affecting cellular interactions and also contributes to a diffusion layer that impedes the permeation and release of prednisolone phosphate. Additionally, proteins can serve as an acceptor phase for poorly soluble drugs [14], such as prednisolone, with profound implications for the conversion kinetics of the drug. Therefore, it is imperative to conduct *in vitro* kinetic measurements of protein binding to accurately identify the factors influencing release behavior. This will enable the assessment of permeation-related unbound and bound fractions and facilitate the development of more comprehensive PBB models based on high-resolution *in vitro* data. Such models, with enhanced resolution, are crucial for establishing more accurate correlations.

To quantify the retention of prednisolone phosphate and its metabolites bound to serum proteins during the release process, it is beneficial to perform permeation experiments utilizing membranes with varying pore sizes. It has been established that a membrane with a MWCO of 50 kDa, effectively retains the albumin-bound fraction of drugs [14]. Conversely, a MWCO of 300 kDa allows for the permeation of the albumin-bound drug fraction. Within this experimental setup, two primary sources of error must be acknowledged. Firstly, the potential for plasma proteins to affect membrane permeation through interactions with the dialysis membrane warrants consideration. To mitigate this, permeation studies have been conducted with solutions of the drug in its free form. Furthermore, to evaluate the influence of serum proteins on drug permeation, comparative studies were conducted in PBS at a pH of 7.4, supplemented with BSA at varying concentrations: 0 g/L, 4 g/L, 20 g/L, and 35 g/L.

Expectedly, in the absence of proteins, the permeation profiles were very similar for both membranes (refer to **Figure 3a**). Increasing protein concentrations led to a retention of the protein-bound fraction and delayed permeation (**Figure 3b-d**). At a concentration of 35g/L, approximately 80% of the drug permeated through the 50 kDa membrane. Such a delay in drug transfer was also reflected by a change in membrane permeation rate constants with increasing protein concentration (refer to **Table 4**).

Table 4 Membrane permeation constant (Km), calculated for drug permeation experiment conducted in various conditions using PT-DR mounted with either 50kDa or 300kDa cellulose ester membrane.

Condition	50kDa (×10cm^2/hr)	300Kda (×10cm^2/hr)
PBS	0.786 ± 0.019	0.872 ± 0.134
PBS + 4g/L BSA	0.766 ± 0.088	0.836 ± 0.049
PBS + 20g/L BSA	0.59 ± 0.171	0.708 ± 0.113
PBS + 35g/L BSA	0.323 ± 0.064	0.44 ± 0.024

The combined approach of investigating the impact of proteins on plasma protein binding and release has been illustrated in **Figure 3e**. On the left, the diagram highlights the process of drug complexation by serum proteins. In the *in vivo* setting, the formation of a protein-bound fraction is anticipated to reduce both tissue exposure and the pharmacological effectiveness of the drug. This effect is expected to be less pronounced during the early phase, as protein binding unfolds over a relatively extended period. The kinetics of free drug permeation through the dialysis membrane

575 are altered as well suggesting the importance of protein-membrane interaction as an
576 analytical error source (**Figure 3e**). This challenge can be addressed by comparing
577 the permeation rates across membranes with two distinct pore sizes, offering a method
578 to quantify the effect of these interactions (refer to **Table 4**).

579 A second source of error is the changing permeability of dialysis membrane over time
580 [14]. Prior investigations have highlighted that the time window for kinetic
581 measurements of drug-protein transfer should be limited to 8hr [14], beyond which
582 swelling of the membrane material in the PTDR significantly affects protein
583 permeation. Therefore, all measurements were conducted over 6 hr to ensure that
584 changes in the membrane permeation rate do not influence the results.

585 To evaluate the impact of protein concentration on the binding kinetics, we assessed
586 drug permeation at multiple concentrations, calculating the percentage of drug
587 retention. Finally, the retention data was then extrapolated to a physiological serum
588 concentration of 40 g/L (**Figure 3f**). With time the drug retention was found to increase.
589 On average about 10% of the released prednisolone phosphate is bound to proteins
590 in the high-shear *in vitro* environment of the PTDR.

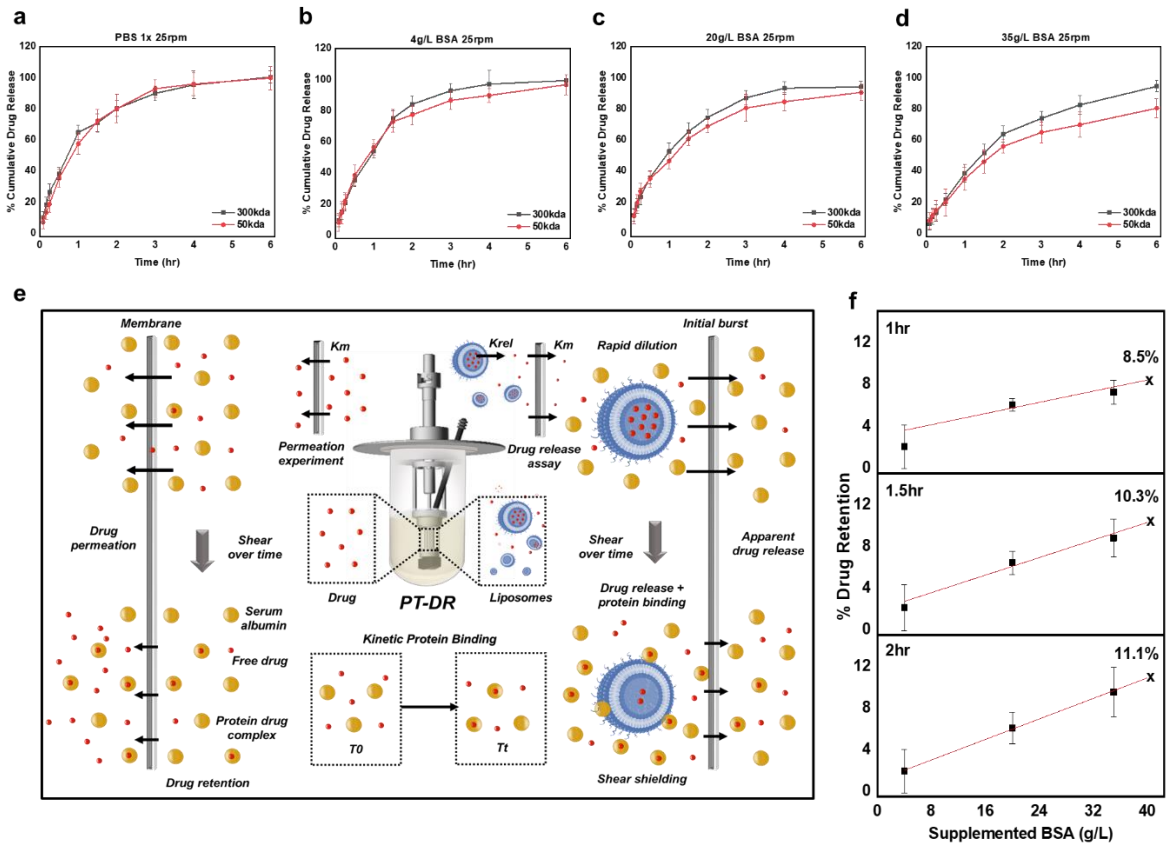

591

592 **Figure 3. Drug permeation profiles in PBS (a), BSA supplemented media in concentrations of 4g/L (b), 20g/L**
593 **(c) and 35g/L (d). The permeation experiment was conducted in 50kDa (Red), and in 300kDa (Black) CE**
594 **membrane in a PT-DR setup (e). The free drug permeation across the membrane is altered in the presence**
595 **of serum components, leading to retention. Upon release, the drug diffuses across the liposomal bilayer**
596 **at a defined rate (K_{rel}) followed by membrane permeation (K_m), in the presence of shear occurs an initial**
597 **burst. The performance is measured as the apparent drug release, influenced by shear and media**
598 **composition. An interplay of serum proteins and shear leads to increased interparticle collisions and shear**
599 **shielding by serum proteins. The kinetic protein binding (f) is calculated by permeation difference across**
600 **50kDa and 300kDa CE membrane over time in the presence of varied protein concentrations, this has been**
601 **extrapolated to physiological concentration (40g/L).**

602 On the right, **Figure 3e** depicts the protective role of the serum protein corona around
603 liposomal prednisolone phosphate, demonstrating their impact on inter-liposomal
604 collisions through shear shielding. This protein corona formation thus acts as a
605 safeguard for the integrity of the liposomal delivery system. These aspects will be
606 discussed in the later sections. Regrettably, the lack of corresponding *in vivo* data
607 inhibits the formulation of definitive conclusions about the applicability of our
608 observations on the role of serum proteins in *in vivo* settings. Nonetheless, it is highly
609 probable that the phenomena observed *in vitro* also manifest *in vivo*, providing
610 valuable insights into the complex mechanisms governing the drug release process.

611 *6.3.2 Liposomal stability*

The physical stability of the carrier system was evaluated using NTA following a 1000-fold dilution of the dispersion. To adjust for the presence of serum proteins in the samples, background measurements were conducted. **Figure 4a** displays the measurement of liposomes in the absence of serum background, where significantly higher concentrations were noted. Selection of relevant particle traces was based on their intensity and concentration. An initial slight increase in the average particle size was noted after 24 hours. This is likely due to the adsorption of serum components and confirms the formation of the protein corona [42,43]. It was followed by a more pronounced increase at prolonged incubation times (48 and 96 hours, as illustrated in **Figure 4b**) , suggesting a potential rearrangement of the lipid bilayer in response to continuous shear [44]. The minimal difference in particle size increase with serum concentrations above 50% suggests a potential surface saturation. A slight increase in particle size was observed with PBS, indicating negligible adsorption on the surface and thus primarily reflecting the influence of shear. Overall, the formulation demonstrated sufficient stability throughout the duration of the *in vitro* release kinetics experiment.

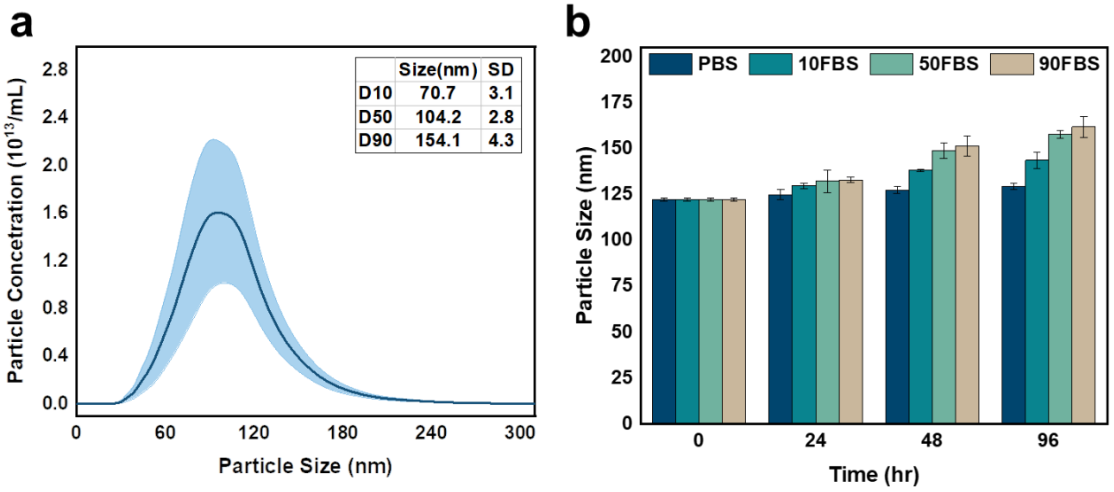

Figure 4: Physicochemical characterization of PLP, with D10, D50, and D90 measured using Nanoparticle Tracking Analysis (NTA NS300, Malvern Panalytical, Malvern, UK) (A). Liposomes characterized for particle size (B) over time in different media compositions, PBS supplemented with FBS (10%), FBS (50%), and FBS (90%).

6.4 Performance predictive assay

Liposomal prednisolone phosphate, like other nanomedicines, circulates in the bloodstream in a pharmacologically inactive form. The pharmacological effects and mode of action are critically determined by the fraction of the drug released either

before or after accumulation at the target site. Clinical pharmacokinetics are typically measured in the plasma, making this the most suitable environment for establishing clinically relevant release test methods. While further investigations into the mode of action at the target site are essential for advancing a drug product, the current work focuses on developing and optimizing release test methods with enhanced biopredictive capabilities.

Although numerous physiological parameters come into play, the *in vitro* release setup emphasizes the most likely rate-limiting steps in the *in vivo* release. Media and apparatus are vital to replicating selected aspects of the physiological environment, ensuring accurate simulation of microenvironmental conditions. For instance, hydrodynamic shear can compromise liposomal integrity, thereby initiating the release of the encapsulated drug. Concurrently, the phenomenon of shear shielding, resulting from protein adsorption on liposome surfaces, may also influence release dynamics. *In silico* deconvolution of the PK was instrumental in estimating the *in vivo* drug release, laying the groundwork for the development of a performance-predictive assay for liposomal prednisolone phosphate. Subsequently, variations in the *in vitro* test conditions and their resulting release profiles are systematically compared to the *in vivo* release using a DoE approach. This comparison aims to delineate the optimal conditions for *in vitro* release.

6.4.1 Optimization of predictive power

The PTDR (**Figure 5a**) enables the measurement of the drug release from liposomal prednisolone phosphate in a well-defined environment. As compared to other dialysis-based methods, the shear rate in the donor chamber can be accurately controlled by altering the stirring rate. In addition to changing this parameter, other independent variables were introduced. The fishbone diagram (**Figure 5b**) outlines the variables investigated using an L-optimal design (refer to **Figure 5c**). A total of 21 drug release experiments were conducted.

The composition of the release media was altered by supplementing PBS (pH 7.4, **Figure 5d**) with varying concentrations of FBS and BSA. The buffer system mimics the pH and osmolarity of the physiological setting. Serum comprises a variety of proteins and enzymes involved in the dephosphorylation of the drug as well as the degradation of lipid components.

Serum concentrations were examined at several levels, including 10% (pH 7.4, **Figure 5e**), 50% (**Figure 5f**), and 90% **Figure 5g**). Past research has shown that biopredictive methods necessitate a specific serum background level [8,13,45]. Additionally, it is widely recognized that albumin functions as a carrier protein in the drug release process. Consequently, we added BSA (**Figure 5h-j**), which provides binding sites for numerous drug molecules, yet lacks the enzymatic activity found in serum.

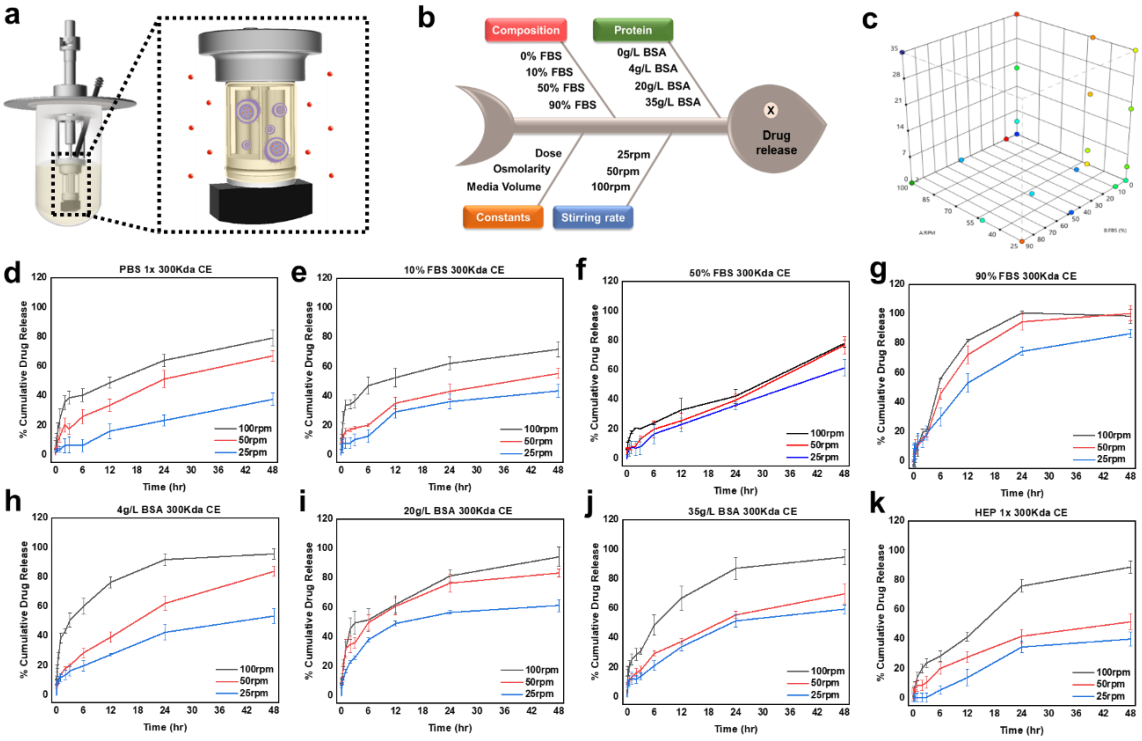

Figure 5. Quality-by-design based development of biorelevant drug release assay using PT-DR (A) by defining independent variable using fishbone diagram (B). The manufactured liposomes were tested using PT-DR setup (A), in various test conditions by design of experiments (C). The plots for cumulative drug release testing for various test conditions including PBS (D), supplemented with FBS (E, F, G) and BSA (H, I, J) or changing to a non-ionic buffer system (K).

One concern during the design of the study was the potential impact of elevated phosphate concentrations on the release of prednisolone phosphate, as the dephosphorylation could be hindered by a strong phosphate background. To address this, we also tested the release in HEPES buffer (**Figure 5k**).

The shear rate significantly influences intravenously administered delivery systems, which experience consistent distribution across a narrow capillary network at varying velocities. The PT-DR system provides a high-shear environment, and the shear stress was adjusted across three levels (25-100 rpm) to refine the release conditions. The different stirring rates are highlighted in different colors (refer to the red, blue, and

black solid lines in **Figure 5d-k**). We focused on examining the effects of shear and the shear-shielding properties of proteins. This involves exploring the potential interaction between the stirring rate and protein concentration, regardless of the protein type. This will be discussed in the later section. The fraction released comprised of both, prednisolone phosphate and prednisolone. Based on a common three-point specifications framework, target responses included the time of release at 5% (T-5%), 20% (T-20%), and 40% release (T-40%). These were compared to the *in vivo* release obtained by deconvolution of the PK. The release was monitored over 48hr.

6.4.2 The interplay of shear and media composition over release performance

Elevated shear rates accelerated the release, potentially due to the accelerated diffusion of drug molecules and the rising number of collision events in the donor chamber. A change in the medium composition may also trigger the release of lipid components from the liposomes as well as the degradation of the carrier material. However, the shape of the release curve was retained. This suggests the same release mechanism at varying conditions and is the desired aim of *in vitro* accelerated conditions. The interplay of shear and media composition was studied across the design space. Time-dependent trends were observed across various release media (**Figure 5d-k**).

The early phase

In the early release phase, an initial 'burst effect' was noted, characterized by rapid drug diffusion immediately following dose administration. This phenomenon, more pronounced at higher shear rates, significantly influences the early release phase (from T-5% to T-20%). Such a burst effect is often indicative of potential quality issues. When BSA or FBS were added, only minimal responses to varying stirring rates were observed at T-5%. This observation was further corroborated by the 3D response surface plots, which indicated that during the early phase (T-5%), increases in BSA concentrations and shear rates did not markedly impact drug release (**Figure 6, a, d, blue zone**). In the case of FBS, a weak response was observed at high serum concentrations and shear rates only (**Figure 6, b and e, green zone**). Among the various factors influencing drug release from liposomes, two processes are particularly rapid following the injection into the donor chamber: the diffusion of the drug into the

medium, and the adsorption of proteins onto the liposome surfaces. The adsorption of proteins is likely to result in delayed drug release, primarily due to the formation of a progressively thicker diffusion boundary layer. This layer acts as a barrier, slowing the diffusion of the drug from the liposome to the external environment. This could be the reason for this slight delay. While the residuals plot shows a good correlation, indicating an optimal data fit (**Figure 6c**), the predictive power (**Figure 6f**) was poor due to the non-significant performance differences. With increasing shear, a burst effect is observed at T-5% and T-20% in almost all experiments, which is slightly compensated by increasing protein and serum concentrations. Shear shielding was most pronounced with media comprising 90% FBS. Furthermore, this shear shielding effect is pronounced in the T-20% zone. Despite higher shear, the shape of various release profiles is almost identical. This is also evident with media comprising 50% FBS. Overall, T-5% is a relatively insensitive parameter and does not exhibit a considerable response to variations in shear.

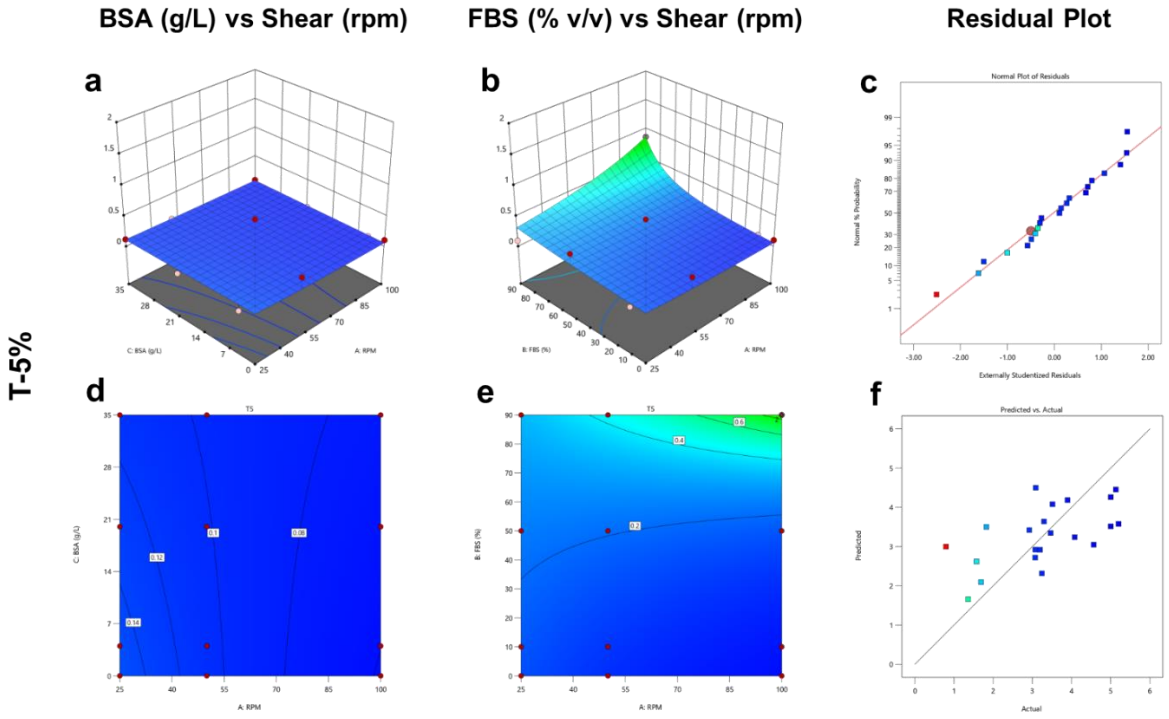

Figure 6. Response surface optimization plot for assessing the interplay between serum components (BSA, %g/L and FBS, % v/v) and shear (rpm) at early phase of release profile represented by T-5%. The 3D response surface plots for BSA vs Shear (a) and FBS vs Shear (b) and its respective contour plots (d , e). The residual plots for model fits (c) and predicted vs observed/actual (f) show the adequacy of model design and accuracy of predictions/extrapolations.

The intermediate phase

The intermediate stage, spanning from T-20% to T-40%, offers the clearest insight into the fundamental release mechanism. In the *in vivo* setting, this period predominantly impacts circulation time and disposition performance. While the burst effect often correlates with safety concerns in follow-on products, efficacy is largely determined by the efficiency of drug delivery. Therefore, the intermediate to late stages are important indicators regarding the safety and efficacy of the formulation. It is significantly influenced by the shear and with a pronounced burst effect. As indicated by the response surface plots, at zero to low concentrations of BSA, an increase in shear stress from 25rpm to 100rpm (**Figure 7a and d, blue zone**) significantly reduces the time to reach 20% release (T-20%). This suggests a reduced interaction with the dynamic protein corona or a decrease in the shear shielding by proteins. This effect is further pronounced with FBS (**Figure 7b and e, yellow zone**) at T-20% to T-40% and could be due to a saturation of protein-binding surfaces or agglomeration of media components *in vitro*. Optimal model fit (**Figure 7c**), and predictive power (**Figure 7f**) were observed for the model.

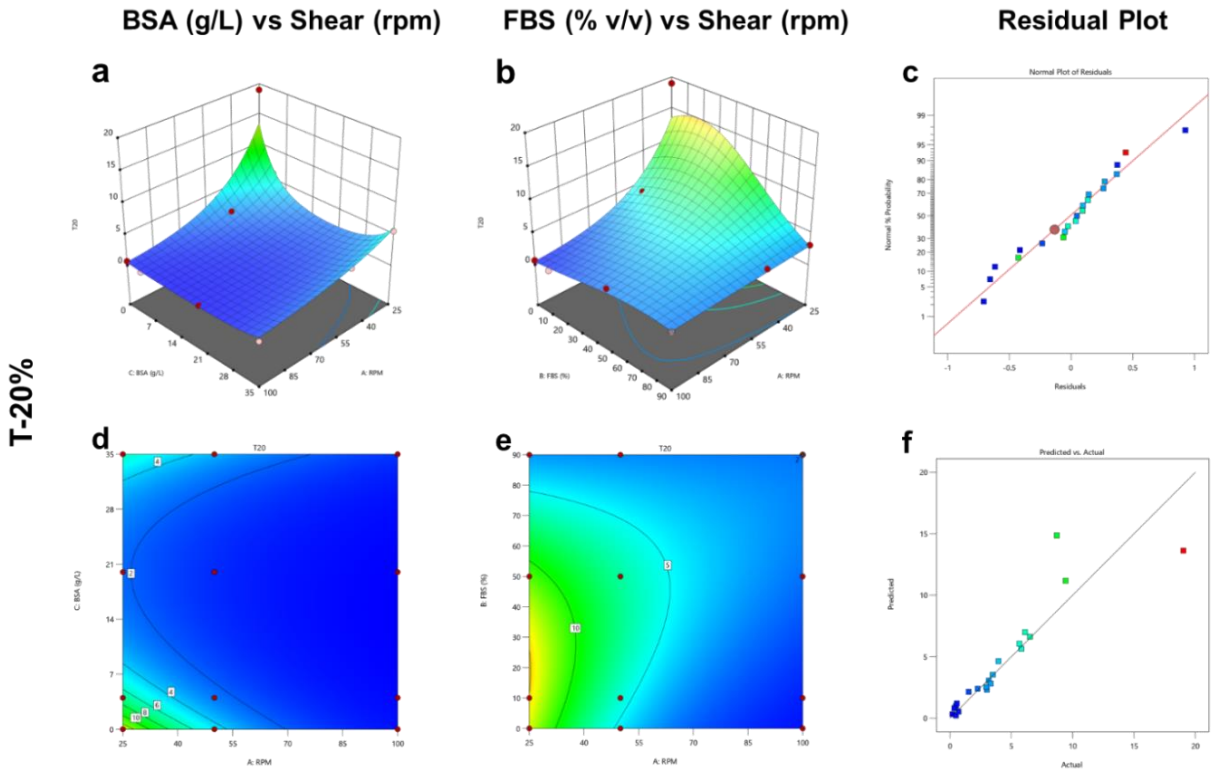

Figure 7. Response surface optimization plot for assessing the interplay between serum components (BSA, %g/L and FBS, % v/v) and shear (rpm) at intermediate phase of release profile represented by T-20%. The 3D response surface plots for BSA vs Shear (a) and FBS vs Shear (b) and its respective contour plots (d, e). The residual plots for model fits (c) and predicted vs observed/actual (f) show the adequacy of model design and accuracy of predictions/extrapolations.

The late phase

T-40% and beyond represents the late stage of the release and is indicative of the overall release performance of the formulation. It provides information on the remaining circulating fraction which is mainly responsible for drug targeting effects.

Consequently, the increasing shear has little to no influence. However, the shear shielding is actually lowered with constant high shear, corresponding to reduced interaction of serum components with liposomes. Therefore, in the presence of media supplemented with BSA, higher protein concentrations are not in line with the shear shielding effect observed with serum (**Figure 8a, d**).

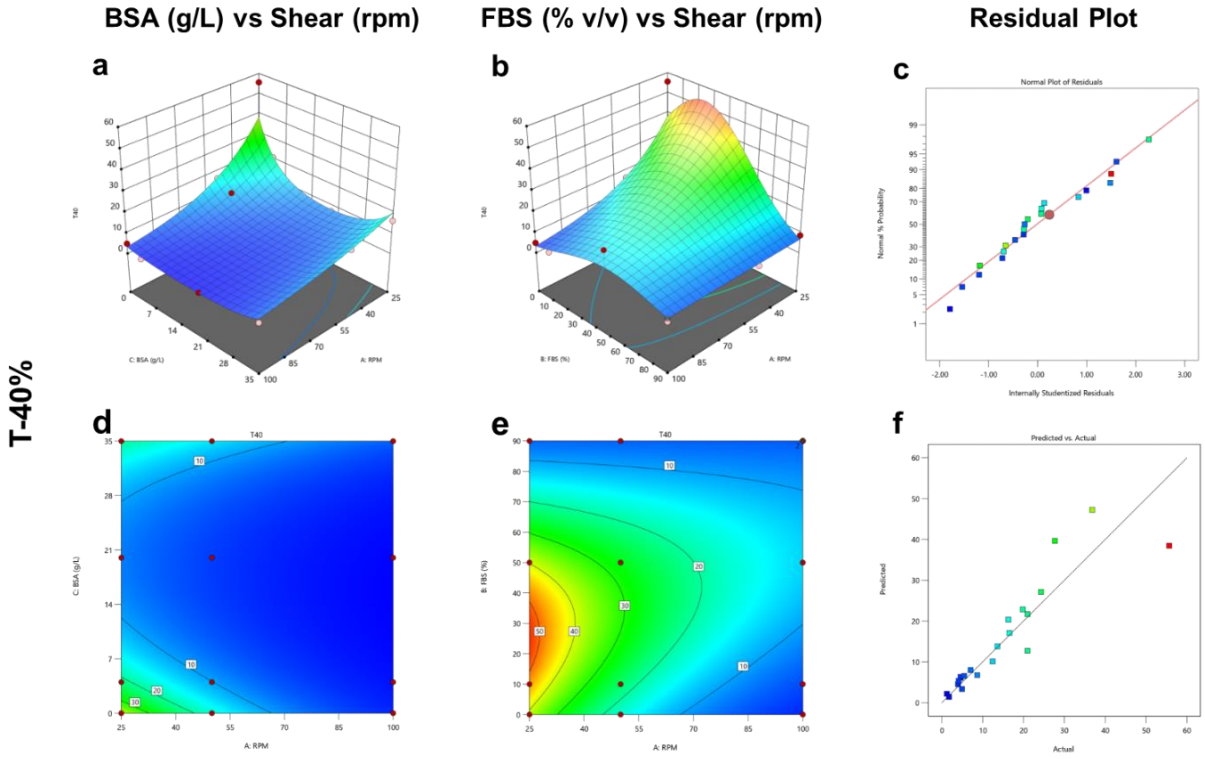

Figure 8. Response surface optimization plot for assessing the interplay between serum components (BSA, %g/L and FBS, % v/v) and shear (rpm) at late phase of release profile represented by T-40%. The 3D response surface plots for BSA vs Shear (a) and FBS vs Shear (b) and its respective contour plots (d , e). The residual plots for model fits (c) and predicted vs observed/actual (f) show the adequacy of model design and accuracy of predictions/extrapolations.

Using 3-D response surface plots a similar trend was observed, and the shear shielding by media components as described above is significant with increasing incubation time and increased interaction at low shear (**Figure 8a, d, green zone**). A significant impact was observed with low to intermediate shear and 50% FBS-supplemented media which is in line with the hypothesis stated above. Shear shielding arises from the formation of a protein corona, which acts as a compressible buffer

between the liposomal carriers, thereby affecting the release dynamics of the encapsulated drug. These effects are more pronounced at lower stirring rates and wear off at higher shear for both, BSA and FBS (**Figure 8b, e, red and yellow zone**). As a result of the interplay of shear and serum components a certain shear shielding effect is observed. Such shear shielding impacts the performance drastically in the intermediate phase, from T-5% to T20%, where most adsorption of proteins on surface of nanocarrier takes place with the sufficient time for incubation. The model fits were found to be good (**Figure 8c**) with excellent predictability (**Figure 8f**) at response T-40%.

Such an investigation is an interesting finding for establishing a biorelevant release testing condition. The interplay of shear shielding with increasing concentration of serum components and incubation time is a dynamic process, which is important to be assessed in a dynamic study to set up the real biorelevant release conditions for nanoparticles. This unique interplay was studied with the QbD pertaining to influence of independent variable on quality attributes (T-5%, T-20% and T-40%).

6.4.3 Optimal biorelevant conditions

The interplay of shear and blood components was assessed to identify biopredictive release conditions for liposomal prednisolone phosphate . Based on the finding presented above, as compared to FBS, BSA has only little shear shielding effects, and does not lead to a sufficient prediction of the *in vivo* effects. Therefore, FBS was considered essential in designing biopredictive media. They exhibit adequate discrimination in the early (up to T-5%), intermediate (up to T-20%), and late phase (T40%). The desirability plot (**Figure 9a**) suggests a medium comprising 50% of FBS and a stirring rate of 50 rpm as most beneficial for the testing of liposomal prednisolone phosphate formulations. T5% (**Figure 9b**), however, is relatively insensitive, potentially due to analytical limitations. The burst effect is more apparent in T-20% (**Figure 9c**). T-20% and T-40% (**Figure 9d**) suggest that using 50% FBS brings the release profile in close alignment with the *in vivo* release.

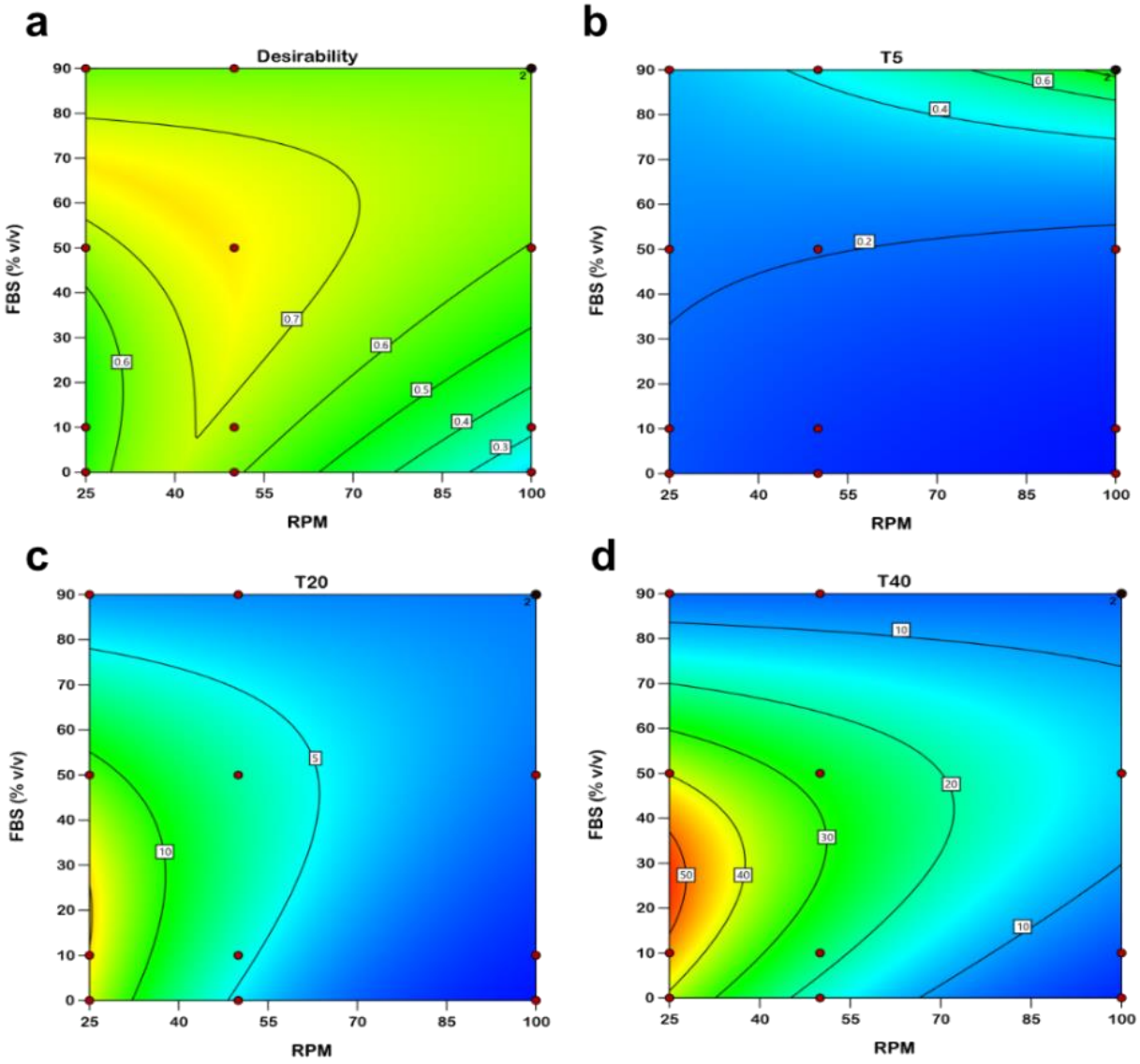

Figure 9. Optimization of Analytical QbD model for assessing the biorelevant conditions. The desirability plot (a) suggest, highest desirability at 50rpm and 50% FBS supplementation. The optimization was carried across early, T-5% (b), intermediate, T-20% (c), T-40%, late phase (d) of drug release. Compared to deconvolution performance from *in silico* modeling, the desirability was computed. The blue and red zone represent higher difference between deconvolution and observed data. The green zone represent the lower difference.

7. Conclusion

This study presents an effective combinatorial approach for designing biopredictive drug release methods for liposomal prednisolone phosphate, incorporating the DeCODe model to align our findings with *in vivo* data and define a design space. Our investigation reveals the critical role of protein adsorption, metabolism, and shear forces in influencing drug release and liposomal stability, with the effect of serum components being predominantly linked to shear rather than direct drug-protein interactions. This is likely due to the high aqueous solubility of prednisolone

phosphate. Notably, the type of protein, whether albumin or FBS, significantly impacts the release, with FBS exerting a more pronounced effect during the extended release phases. This delay in release corresponds to literature reports indicating the formation of a protein corona that serves as an additional diffusion layer on the surface of liposomes. Alternatively, it could be attributed to a shear shielding effect that protects the integrity of the liposomes. Our study further refines analytical QbD strategies to mirror physiological protein concentrations accurately, and identifies potential errors in dialysis-based assays. Additionally, we demonstrated that conditions of intermediate shear (50 rpm) in PBS (10mM, pH 7.4) supplemented with 50% v/v FBS are optimal for evaluating the performance of NanoCort®.

8. Acknowledgements

The authors acknowledge the Ministry of Education of Singapore (MoE Tier1 A-8001991-00-00, Startup A-0004627-00-00) and the National University of Singapore NanoNASH Program (NUHSRO/2020/002/NanoNash/LOA) for financial support.

9. References

[1] U. Bulbake, S. Doppalapudi, N. Kommineni, W. Khan, Liposomal Formulations in Clinical Use: An Updated Review, Pharmaceutics. 9 (2017). https://doi.org/10.3390/PHARMACEUTICS9020012.

[2] G. Singhvi, V.K. Rapalli, S. Nagpal, S.K. Dubey, R.N. Saha, Nanocarriers as Potential Targeted Drug Delivery for Cancer Therapy, in: Nanosci. Med., Springer, Cham, 2020: pp. 51–88. https://doi.org/10.1007/978-3-030-29207-2_2.

[3] Y. Barenholz, Doxil® — The first FDA-approved nano-drug: Lessons learned, J. Control. Release. 160 (2012) 117–134. https://doi.org/10.1016/J.JCONREL.2012.03.020.

[4] T.G. Agnihotri, A. Alexander, M. Agrawal, S.K. Dubey, A. Jain, *In vitro-in vivo* correlation in nanocarriers: From protein corona to therapeutic implications, J. Control. Release. 354 (2023) 794–809. https://doi.org/10.1016/J.JCONREL.2023.01.063.

[5] C. Decker, H. Schubert, S. May, A. Fahr, Pharmacokinetics of temoporfin-

loaded liposome formulations: Correlation of liposome and temoporfin blood concentration, J. Control. Release. 166 (2013) 277–285. https://doi.org/10.1016/J.JCONREL.2013.01.005.

[6] F. Jung, L. Nothnagel, F. Gao, M. Thurn, V. Vogel, M.G. Wacker, A comparison of two biorelevant *in vitro* drug release methods for nanotherapeutics based on advanced physiologically-based pharmacokinetic modelling, Eur. J. Pharm. Biopharm. 127 (2018) 462–470. https://doi.org/10.1016/J.EJPB.2018.03.010.

[7] L. Jablonka, M. Ashtikar, G. Gao, F. Jung, M. Thurn, A. Preuß, D. Scheglmann, V. Albrecht, B. Röder, M.G. Wacker, Advanced *in silico* modeling explains pharmacokinetics and biodistribution of temoporfin nanocrystals in humans, J. Control. Release. 308 (2019) 57–70. https://doi.org/10.1016/J.JCONREL.2019.06.029.

[8] S. Nagpal, Y.J.J. Png, J. Malinovskaya, T. Kovshova, P. Jain, S. Naik, A. Khopade, S. Bhowmick, P. Shahi, A. Chakra, A. Bhokari, V. Shah, S. Gelperina, M.G. Wacker, A design-conversed strategy establishes the performance safe space for doxorubicin nanosimilars, ACS Nano. (2023).

[9] J. Shen, D.J. Burgess, *In vitro* dissolution testing strategies for nanoparticulate drug delivery systems: Recent developments and challenges, Drug Deliv. Transl. Res. 3 (2013) 409–415. https://doi.org/10.1007/S13346-013-0129-Z/METRICS.

[10] M. Villa Nova, K. Gan, M.G. Wacker, Biopredictive tools for the development of injectable drug products, Expert Opin. Drug Deliv. 19 (2022) 671–684. https://doi.org/10.1080/17425247.2022.2081682.

[11] L. Nothnagel, M.G. Wacker, How to measure release from nanosized carriers?, Eur. J. Pharm. Sci. 120 (2018) 199–211. https://doi.org/10.1016/J.EJPS.2018.05.004.

[12] M.G. Wacker, X. Lu, M. Burke, Ishai Nir, R. Fahmy, Testing the In-Vitro Product Performance of Nanomaterial-Based Drug Products: View of the USP Expert Panel, (2022). https://doi.org/10.14227/DT290122P6.

[13] H. Modh, D.J. Fang, Y.H. Ou, J.N.N. Yau, T. Kovshova, S. Nagpal, J. Knoll, C.M.

888 Wallenwein, K. Maiti, S. Bhowmick, S. Gelperina, G. Pastorin, M.G. Wacker,
889 Injectable drug delivery systems of doxorubicin revisited: *In vitro-in vivo*
890 relationships using human clinical data, Int. J. Pharm. 608 (2021) 121073.
891 https://doi.org/10.1016/J.IJPHARM.2021.121073.

892 [14] C.M. Wallenwein, M.V. Nova, C. Janas, L. Jablonka, G.F. Gao, M. Thurn, V.
893 Albrecht, A. Wiehe, M.G. Wacker, A dialysis-based *in vitro* drug release assay
894 to study dynamics of the drug-protein transfer of temoporfin liposomes, Eur. J.
895 Pharm. Biopharm. 143 (2019) 44–50.
896 https://doi.org/10.1016/J.EJPB.2019.08.010.

897 [15] L. Jablonka, M. Ashtikar, G.F. Gao, M. Thurn, H. Modh, J.W. Wang, A. Preuß,
898 D. Scheglmann, V. Albrecht, B. Röder, M.G. Wacker, Predicting human
899 pharmacokinetics of liposomal temoporfin using a hybrid *in silico* model, Eur. J.
900 Pharm. Biopharm. 149 (2020) 121–134.
901 https://doi.org/10.1016/J.EJPB.2020.02.001.

902 [16] C. Janas, M.P. Mast, L. Kirsamer, C. Angioni, F. Gao, W. Mäntele, J. Dressman,
903 M.G. Wacker, The dispersion releaser technology is an effective method for
904 testing drug release from nanosized drug carriers, Eur. J. Pharm. Biopharm. 115
905 (2017) 73–83. https://doi.org/10.1016/j.ejpb.2017.02.006.

906 [17] T. Kovshova, N. Osipova, A. Alekseeva, J. Malinovskaya, A. Belov, A. Budko,
907 G. Pavlova, O. Maksimenko, S. Nagpal, S. Braner, H. Modh, V. Balabanyan,
908 M.G. Wacker, S. Gelperina, Exploring the Interplay between Drug Release and
909 Targeting of Lipid-Like Polymer Nanoparticles Loaded with Doxorubicin, Mol.
910 2021, Vol. 26, Page 831. 26 (2021) 831.
911 https://doi.org/10.3390/MOLECULES26040831.

912 [18] X. Shao, C. Shi, S. Wu, F. Wang, W. Li, Review of the pharmacokinetics of
913 nanodrugs, Nanotechnol. Rev. 12 (2023). https://doi.org/10.1515/NTREV-2022-
914 0525/ASSET/GRAPHIC/J_NTREV-2022-0525_FIG_004.JPG.

915 [19] M.P. Mast, H. Modh, C. Champanhac, J.W. Wang, G. Storm, J. Krämer, V.
916 Mailänder, G. Pastorin, M.G. Wacker, Nanomedicine at the crossroads – A quick
917 guide for IVIVC, Adv. Drug Deliv. Rev. (2021) 113829.
918 https://doi.org/10.1016/J.ADDR.2021.113829.

[20] S. Nagpal, S. Braner, H. Modh, A.X.X. Tan, M.P. Mast, K. Chichakly, V. Albrecht, M.G. Wacker, A physiologically-based nanocarrier biopharmaceutics model to reverse-engineer the *in vivo* drug release, Eur. J. Pharm. Biopharm. 153 (2020) 257–272. https://doi.org/10.1016/J.EJPB.2020.06.004.

[21] A.A. Halwani, Development of Pharmaceutical Nanomedicines: From the Bench to the Market, Pharm. 2022, Vol. 14, Page 106. 14 (2022) 106. https://doi.org/10.3390/PHARMACEUTICS14010106.

[22] G. Pastorin, C. Benetti, M.G. Wacker, From *in vitro* to *in vivo*: A comprehensive guide to IVIVC development for long-acting therapeutics, Adv. Drug Deliv. Rev. 199 (2023) 114906. https://doi.org/10.1016/J.ADDR.2023.114906.

[23] S. Suarez-Sharp, M. Cohen, F. Kesisoglou, A. Abend, P. Marroum, P. Delvadia, E. Kotzagiorgis, M. Li, A. Nordmark, N. Bandi, E. Sjögren, A. Babiskin, T. Heimbach, S. Kijima, H. Mandula, K. Raines, P. Seo, X. Zhang, Applications of Clinically Relevant Dissolution Testing: Workshop Summary Report, AAPS J. 20 (2018) 1–14. https://doi.org/10.1208/S12248-018-0252-3/METRICS.

[24] J.M. Metselaar, M.H.M. Wauben, J.P.A. Wagenaar-Hilbers, O.C. Boerman, G. Storm, Complete remission of experimental arthritis by joint targeting of glucocorticoids with long-circulating liposomes, Arthritis Rheum. 48 (2003) 2059–2066. https://doi.org/10.1002/ART.11140.

[25] E.A.W. Smits, J.A. Soetekouw, H. Vromans, *In vitro* confirmation of the quantitative differentiation of liposomal encapsulated and non-encapsulated prednisolone (phosphate) tissue concentrations by murine phosphatases, Http://Dx.Doi.Org/10.3109/08982104.2013.850593. 24 (2014) 130–135. https://doi.org/10.3109/08982104.2013.850593.

[26] Tools & Projects, (n.d.). http://www.anim.med.kyoto-u.ac.jp/nbr/tools.aspx (accessed May 16, 2022).

[27] R.P. Brown, M.D. Delp, S.L. Lindstedt, L.R. Rhomberg, R.P. Beliles, Physiological Parameter Values for Physiologically Based Pharmacokinetic Models:, Http://Dx.Doi.Org/10.1177/074823379701300401. 13 (2016) 407–484. https://doi.org/10.1177/074823379701300401.

[28] C.M. Mendel, The Free Hormone Hypothesis: A Physiologically Based Mathematical Model, Endocr. Rev. 10 (1989) 232–274. https://doi.org/10.1210/EDRV-10-3-232.

[29] X. Li, D.C. Dubois, R.R. Almon, W.J. Jusko, Physiologically-Based Pharmacokinetic Modeling Involving Nonlinear Plasma and Tissue Binding: Application to Prednisolone and Prednisone in Rats, J. Pharmacol. Exp. Ther. 375 (2020) 385–396. https://doi.org/10.1124/JPET.120.000191.

[30] T. Siegal, A. Horowitz, A. Gabizon, Doxorubicin encapsulated in sterically stabilized liposomes for the treatment of a brain tumor model: biodistribution and therapeutic efficacy, J. Neurosurg. 83 (1995) 1029–1037. https://doi.org/10.3171/JNS.1995.83.6.1029.

[31] H.B. Lee, M.D. Blaufox, Blood Volume in the Rat, J. Nucl. Med. 26 (1985) 72–76. https://jnm.snmjournals.org/content/26/1/72 (accessed December 17, 2023).

[32] E.A.W. Smits, J.A. Soetekouw, E.H.E. Pieters, C.J.P. Smits, N. de Wijs-Rot, H. Vromans, The availability of drug by liposomal drug delivery: Individual kinetics and tissue distribution of encapsulated and released drug in mice after administration of PEGylated liposomal prednisolone phosphate, Invest. New Drugs. 37 (2019) 890. https://doi.org/10.1007/S10637-018-0708-4.

[33] E.A.W. Smits, J.A. Soetekouw, P.F.A. Bakker, B.J.H. Baijens, H. Vromans, Plasma, blood and liver tissue sample preparation methods for the separate quantification of liposomal-encapsulated prednisolone phosphate and non-encapsulated prednisolone, J. Liposome Res. 25 (2015) 46–57. https://doi.org/10.3109/08982104.2014.928887.

[34] S. Hansmann, A. Darwich, … A.M.-J. of P., undefined 2016, Forecasting oral absorption across biopharmaceutics classification system classes with physiologically based pharmacokinetic models, Academic.Oup.Com. (n.d.). https://academic.oup.com/jpp/article-abstract/68/12/1501/6128245 (accessed October 23, 2021).

[35] A. Margolskee, A. Darwich, L. Aarons, A. Galetin, Rostami-Hochaghan, S. Hammarberg, M. Hilgendorf, C. Johansson, P. Karlsson, E. Murphy, C. Thorn,

H. Yasin, Nicolas, O. Ramusovic, S. Xu, IMI–Oral biopharmaceutics tools project–Evaluation of bottom-up PBPK prediction success part 2: An introduction to the simulation exercise and overview of results, Elsevier. (n.d.). https://doi.org/10.1016/j.ejps.2016.10.036.

[36] R. Obach, J. Baxter, T. Liston, … B.S.-… of P. and, undefined 1997, The prediction of human pharmacokinetic parameters from preclinical and *in vitro* metabolism data, ASPET. 283 (1997) 46–58. https://jpet.aspetjournals.org/content/283/1/46.short (accessed October 23, 2021).

[37] E. Medicines Agency, Committee for Medicinal Products for Human Use (CHMP) Guideline on the reporting of physiologically based pharmacokinetic (PBPK) modelling and simulation, (2018). www.ema.europa.eu/contact (accessed October 28, 2021).

[38] Z. Li, T. Kovshova, J. Malinovskaya, M. Valikhov, P. Melnikov, N. Osipova, O. Maksimenko, N. Dhakal, A. Chernysheva, V. Chekhonin, S. Gelperina, M.G. Wacker, Modeling the Drug delivery Lifecycle of PLG Nanoparticles Using Intravital Microscopy, Small. (2023) 2306726. https://doi.org/10.1002/SMLL.202306726.

[39] K. Yalcin Arga, A. Keshavarzi Arshadi, E. Gov, M.G. Wacker, V.M. Nova, N. Scy, M. Villa Nova, T. Ping Lin, S. Shanehsazzadeh, K. Jain, S. Cheng Yong Ng, R. Wacker, K. Chichakly, Nanomedicine Ex Machina: Between Model-Informed Development and Artificial Intelligence, Front. Digit. Heal. | Www.Frontiersin.Org. 4 (2022) 799341. https://doi.org/10.3389/fdgth.2022.799341.

[40] S. Hansmann, A. Darwich, A. Margolskee, L. Aarons, J. Dressman, Forecasting oral absorption across biopharmaceutics classification system classes with physiologically based pharmacokinetic models, J. Pharm. Pharmacol. 68 (2016) 1501–1515. https://doi.org/10.1111/JPHP.12618.

[41] M.N. Dimitrova, H. Matsumura, A. Dimitrova, V.Z. Neitchev, Interaction of albumins from different species with phospholipid liposomes. Multiple binding sites system, Int. J. Biol. Macromol. 27 (2000) 187–194.

https://doi.org/10.1016/S0141-8130(00)00123-9.

[42] H. Lee, R.G. Larson, Adsorption of Plasma Proteins onto PEGylated Lipid Bilayers: The Effect of PEG Size and Grafting Density, Biomacromolecules. 17 (2016) 1757–1765. https://doi.org/10.1021/ACS.BIOMAC.6B00146/ASSET/IMAGES/LARGE/BM-2016-00146H_0010.JPEG.

[43] Y. Yokouchi, T. Tsunoda, T. Imura, H. Yamauchi, S. Yokoyama, H. Sakai, M. Abe, Effect of adsorption of bovine serum albumin on liposomal membrane characteristics, Colloids Surfaces B Biointerfaces. 20 (2001) 95–103. https://doi.org/10.1016/S0927-7765(00)00176-4.

[44] S. Karaz, E. Senses, Liposomes Under Shear: Structure, Dynamics, and Drug Delivery Applications, Adv. NanoBiomed Res. 3 (2023) 2200101. https://doi.org/10.1002/ANBR.202200101.

[45] M.P. Mast, H. Modh, J. Knoll, E. Fecioru, M.G. Wacker, An update to dialysis-based drug release testing—data analysis and validation using the pharma test dispersion releaser, Pharmaceutics. 13 (2021) 2007. https://doi.org/10.3390/PHARMACEUTICS13122007/S1.